Even-Odd Differences and Shape Deformation of Metal Clusters

Sci. Rep. RITU A39 (1993) pp. 39-42
No. 1, December 1993

Even-Odd Differences and Shape Deformation of Metal Clusters

Hidetoshi Nishioka and Yoshio Takahashi [1]
Department of Physics, Konan University, Kobe 658, Japan
[1] *Faculty of General Education, Yamagata University, Yonezawa, Yamagata-ken 992, Japan*

(Received November 30, 1993)

The relation between even-odd difference of metal cluster and the deformation of equilibrium shape is studied in terms of two different models; (i) tri-axially deformed harmonic oscillator model, (ii) rectangular box model. Having assumed the matter density ρ kept constant for different shapes of a cluster, we can determine the equilibrium shape both for the two models. The enhancement of HOMO-LUMO gap is obtained and it is ascribed to Jahn-Teller effect. Good agreement of the calculated results on ionization potential and the experimental values is obtained.

KEYWORDS: metal cluster, even-odd difference, Jahn-Teller effect, HOMO-LUMO gap, ionization potential

1. Introduction

The origin of even-odd staggering of binding energy of metal cluster has been drawing much attention from many authors[1,2]. Having noticed the shell effect is prominent in the abundance spectrum of metal cluster, it is believed that the shell model provides the basic frame for describing the properties of the system[1,2]. Since the spherical shell model gives highly degenerated single particle spectrum, it is obvious that one fails to obtain finite even-odd difference in the total energy. One can immediately imagine two different sort of models to account for the even-odd difference; pairing model of interacting electrons and free electron gas model in a deformed potential. The absolute values of experimental even-odd difference for ionization potential[3-5] of Na are about 0.2 eV at $N \approx 20$. It seems to be hard to account for these values consistently as the energy gap given by the pairing model. The second model accounts for the even-odd difference as the result of Jahn-Teller distortion. The degeneracy of single particle states is split due to the deformation of equilibrium shape and this brings the origin of the even-odd staggering of the total energy.

Within the framework of the second model, we investigate the even-odd difference and the shape deformation for wide range of cluster size N. The fact that no quartet structure (two teeth of a saw shape are merged into one) is found in observed ionization potential[6,7] of Li and Cu suggest Clemenger's model[8] is not sufficient with respect to Jahn-Teller distortion. Hence we choose two extreme models of free electron gas in (i) quadratically deformed harmonic model (DHOM), and (ii) rectangular box model (RBM). The residual interactions (electron-electron and electron-positive ion) will modify the result, but we assume that their effects have no vital importance to the problem considered here and ignore them. In order to determine the equilibrium shape of a cluster, we further assume that the average electron density ρ is the same among the different shapes for a given N and, furthermore ρ is constant for different cluster sizes.

Under these assumption, we find analytic expressions of the total energy for both of the models as functions of limited set of variables. The lowest total energy, equilibrium shape and other quantities are determined by the condition to minimize the total energy with constant ρ constraint. All of them are expressed in terms of algebraic functions of N, electron configuration ν over the model basis and ρ. Therefore the present models are applicable to both of alkali and noble metal clusters by choosing single parameter ρ appropriately.

In this work, we study the structure of single particle spectrum, shape and ionization potential (IP) of sodium cluster. The brief comparison of theoretical results with experimental data is made for IP.

2. Model

The hamiltonian H for free fermion gas in a potential well U is given

$$H = H_0 + U \tag{1}$$

where $H_0 = (p_1^2 + p_2^2 + p_3^2)/(2m)$. For the potential part, we consider the following two cases;

$$U_H = \frac{m}{2}\left(\omega_1^2 x_1^2 + \omega_2^2 x_2^2 + \omega_3^2 x_3^2\right), \tag{2}$$

$$U_B = \begin{cases} 0 & ; |x_1| \le L_1,\ |x_2| \le L_2,\ |x_3| \le L_3, \\ \infty & ; \text{otherwise}, \end{cases} \tag{3}$$

where U_H and U_B denotes deformed harmonic oscillator potential and rectangular box potential, respectively. The single particle energy spectrum for each model is given as follows;

(i) Deformed Harmonic Oscillator Model (DHOM)

$$\mathcal{E}(\Omega\,;\tilde{n}) = \hbar\sum_j \omega_j\left(n_j + \frac{1}{2}\right) \quad ;\ n_j = 0,\ 1,\ 2,\ \cdots \text{ and } j = 1,2,3$$

where Ω and $\tilde{n}$ is the collective expression of $\omega_1, \omega_2, \omega_3$ and n_1, n_2, n_3 respectively.

(ii) Rectangular Box Model (RBM)

$$\mathcal{E}(\Lambda\,;\tilde{n}) = \sum_j \epsilon(L_j) n_j^2 \quad ; \quad \epsilon(L_j) = \frac{\pi^2\hbar^2}{2m}\frac{1}{4L_j^2}, \quad n_j = 1,\ 2,\ 3,\ \cdots \text{ and } j = 1,2,3$$

where Λ represents L_1, L_2, L_3 and $\tilde{n}$ is just the same abbreviation introduced in the previous model.

For a single particle state n_1, n_2, n_3, the occupation number η of electron can take tone of the values 0, 1 or 2. Let us adopt here a notation $(n_1\ n_2\ n_3)^{\eta}$ by the analogy of spectroscopy in order to represent a configuration of electrons over single particle basis. Then a general configuration ν over such basis can be written as $\nu_1\nu_2\ldots$, where we $\nu_i = (n_1(i)\ n_2(i)\ n_3(i))^{\eta_i}$. We further introduce the notation $N_j(\nu)$ to the sum of quanta over given configuration ν with respect to the x_j-axis

$$N_j(\nu) = \begin{cases} \displaystyle\sum_{\nu_i\in\nu} \eta_i n_j(i) & ;\ \text{DHOM}, \\ & j = 1,2,3 \\ \displaystyle\sum_{\nu_i\in\nu} \eta_i \left(n_j(i)\right)^2 & ;\ \text{RBM}. \end{cases} \tag{4}$$

With these notation, the total energy E of free electron gas with configuration ν is expressed as

$$E(\Xi;\nu) = \begin{cases} \dfrac{\hbar}{2}\displaystyle\sum_{j=1}^{3}\omega_j(2N_j(\nu)+N) & ;\ \text{DHOM}, \\ \displaystyle\sum_{j=1}^{3}\epsilon(L_j)N_j(\nu) & ;\ \text{RBM}, \end{cases} \tag{5}$$

where Ξ denotes Ω for DHOM and Λ for RBM, respectively.

Having formulated the method to fix the equilibrium shape of cluster in the previous section, it is easy to see that the shape can be found by solving the problem to minimize the generalized energy functional $F(\Xi;\nu)$ with respect to the variation of *shape parameter* Ξ

$$F(\Xi;\nu) = H(\Xi;\nu) - \mu\psi(\Xi;\nu)\,, \tag{6}$$

where μ is the Lagrange multiplier of constraint condition $\psi = 0$. Its explicit form of is given

$$\psi(\Xi;\nu) = \rho V(\Xi;\nu) - N = 0\,, \tag{7}$$

where V is the volume of given system and one can calculate theoretically in the present models. For DHOM, we choose it $4\pi R_1(\nu)R_2(\nu)\,R_3(\nu)/\,3$, where $R_j(\nu)$ is the quantum mechanical counterpart of a object having uniform density distribution with sharp surface.[9] We set V as $L_1L_2L_3$ for RBM. Note that $V(\Xi;\nu)$ can be represented in a explicit form of Ξ and $N_j(\nu)$ in both models.

Let us use ξ_j instead of ω_j or L_j for simplicity. The stationary point of F must satisfy the following equations,

$$\begin{cases} \dfrac{\partial F}{\partial \xi_j} = 0 \quad ; \quad (j = 1,\ 2,\ 3)\,, \\ \dfrac{\partial F}{\partial \mu} = 0\,. \end{cases} \tag{8}$$

The "shape parameters" ξ_j and the Lagrange multiplier μ are solved as functions of $N_j(\nu)$, i.e. the equilibrium shape can be expressed in terms of given electron configuration ν. By inserting these expressions into Eq. (5), the minimum total energy E is finally obtained as a function of single variable ν. However many different configurations are possible for given electron number N. Hence the problem reduces to find the special configuration ν which makes $E(\nu)$ be real minimum(-ma) among possible configurations for given N and ρ.

The present approach greatly reduces the amount of calculation to find the real minimum(-ma) compared with the full numerical method.[10] The procedure of the latter is separated in two successive steps; (a) search the equilibrium shape for given configuration by changing "shape parameter", (b) repeat the process (a) by selecting different configurations and decide the real minimum(-ma) among the results. The first step is obviously not necessary to the approach described here, since the result of process (a) has been already given in concrete form.

Various physical quantities depend on cluster size N. Among them, there are interesting quantities which tend to certain non-trivial limiting values at $N \to \infty$. For example, if we define the Fermi energy $\varepsilon_{\rm F}$ of the system as the energy of the highest occupied single particle state, one can show that $\varepsilon_{\rm F}$ is just such quantity in reasonable postulation. By using the asymptotic behaviour of $N_j(\nu)$ for DHOM at large N, one finds

$$\varepsilon_{\rm F} \to \left(\frac{4\pi\rho}{3}\right)^{2/3}\cdot\frac{\hbar^2}{m}\frac{5\sqrt[3]{9}}{4} \quad \text{as} \quad N\to\infty\,. \tag{9}$$

For RBM, it seems to be impossible to find simple analytical relation between $N_j(\nu)$ and N even for closed shell case. But we can calculate the asymptotic value of $\varepsilon_{\rm F}$ by assuming the average density ρ kept constant for large N,

$$\varepsilon_{\rm F} \to \frac{\hbar^2}{2m}\left(3\pi^2\rho\right)^{2/3} \quad \text{as} \quad N\to\infty\,. \tag{10}$$

In this work, we treat a quadrupole shape of cluster in DHOM and a general rectangular parallelopiped shape in RBM, respectively. Since the standard prescription to describe quadrupole deformation has been established,[11] we follow it and introduce the deformation parameters β and γ; once $R_j(\nu)$ has been obtained, these parameters are easily determined.[10] On the other hand, there are no standard method to parametrize RBM. Having noticed that the deformation considered here preserve the "volume" of an object [see Eq. (7)], it is obvious that the shape can be characterized by two parameters. Thus let us adopt the same prescription (use β and γ parametrization) as DHOM case by using L_j instead of R_j.

The theoretical ionization potential of a cluster is roughly estimated by the absolute value of the highest occupied level energy calculated by a suitable method, e.g. Hartree-Fock approximation of the system. Unfortunately both of the potentials considered here have infinite depth and therefore it is impossible to obtain the difference of zero-energy and the highest occupied level. Instead we calculate the first difference of $\varepsilon_{\rm F}(N)$

$$\Delta(\varepsilon_{\rm F};N) := -\left(\varepsilon_{\rm F}(N) - \varepsilon_{\rm F}(N-1)\right)\,, \tag{11}$$

and compare with the experiments. Note that the minus sign in Eq. (11) is necessary because the each value of ε_F is measured from the bottom of the potential, respectively.

3. Calculation

In searching the real minimum, we need to take the whole possible configurations for given N and compare their total energies. The number of possible configurations swells explosively as N increases when we take the space of single particle basis sufficiently large. Therefore we are forced to truncate the basis space into appropriate size by practical reason. Thorough calculation up to $N \approx 100$ shows that it is sufficient to take the model space S which is composed by the full basis of valence shell and upper and lower one major shells around it plus several basis among second upper and lower major shells. Actually we choose further large model space by adding several basis among the third major shells both side of valence shell to the space S. We fix $\rho = 2.652\times10^{-2}$Å^{-3} both of the two model throughout the calculation for sodium cluster. This choice reproduce the bulk Fermi energy of sodium[12] $\varepsilon_F = 3.24$ eV in RBM at large N. We calculate the case of cluster size up to over $N = 440$ for both models.

4. Results

The present approach is powerful compared with the full numerical method of Selby et al.[11], since it gives the new ground state configurations for $N = 16$, 27, 28 and 29 unknown previously. In the following, we will describe the results which are a part of our recent calculation.

4.1 Single particle spectrum and HOMO-LUMO gap

In Fig. 1 shows the calculated single particle spectrum for DHOM. The gross

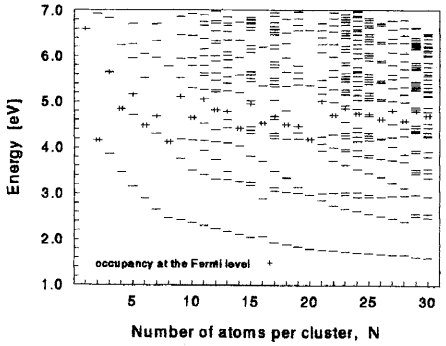

Figure 1: Single particle spectra of sodium clusters.

features are quite similar to those given by Hückel model and molecular dynamical model.[13–15]. The enhancement of HOMO-LUMO gap due to the Jahn-Teller distortion is widely observed. The χ^2 fitting for the enhancement factor to the average level distance around the Fermi surface gives 1.838 (cluster size $N = 41$ to 444). Crossing of single particle orbits due to the deformation are clearly seen. It is worth to point out that the position of the Fermi level shows saw shape as N changes. All of these situations are also observed in rectangular box model.

4.2 Deformation of equilibrium shape

The calculated values of deformation parameters β and γ with DHOM are shown in Figs. 2 and 3. As expected, β deformation grows in the region where particles fill half part of major shell. There often appears hole intruder state in such region, by accompanying a sudden shape change. Although we omit the details, the behavior of N-dependence of the deformation obtained by the model is very similar to the results given by more realistic model.[16].

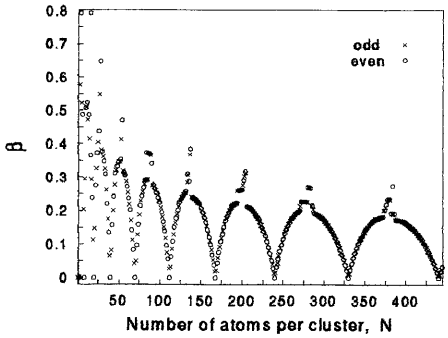

Figure 2: Deformation parameter β of sodium clusters.

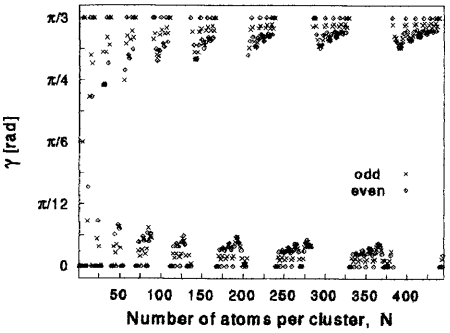

Figure 3: Deformation parameter γ of sodium clusters.

At first glance, γ parameters take relatively small values ($\leq 10°$) except for small N region. Most clusters are regarded as a quasi-axial symmetric objects. But an interesting regularity on N dependence of γ can observed in the fine structures of Fig. 3. In particular the variations in the oblate regions around $N \approx 300$ and 400 are very clear. Each small downward peak pattern shows particle filling process to the degenerate $n_\perp$ multiplet. This shows that tri-axial deformation does not developed well in DHOM and very small amount of triaxiality is sufficient to stabilize the whole system.

On the other hand, the calculate results show rather vague or irregular behavior of β parameter in RBM. The γ values shoe widely scattered patterns between 0 to $\pi/3$ (both figures are omitted). These might be the consequence of sparse level density near the Fermi surface.

4.3 Ionization potential

Having described in Sect. 2, since it is impossible to calculate the ionization potential $IP(N)$ of N-cluster by both of our models, we calculate the first difference $\Delta(\varepsilon_F; N)$ defined by Eq. (11). Roughly speaking, this quantity can be regarded as the first difference of the ionization potential $IP(N) - IP(N-1)$ if we ignore the effect of correlations between electrons. The results are summarized in Fig. 4 for $N = 2$ to 25.

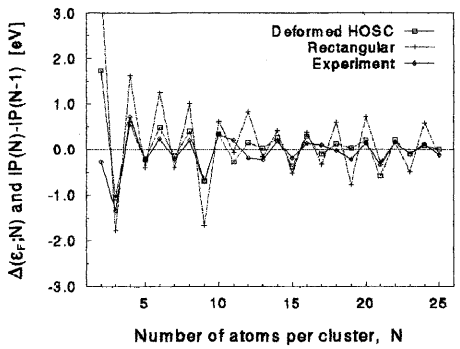

Figure 4: First difference of ionization potential sodium clusters. Experimental data are taken from Refs. 3 – 5.

In calculating $\Delta(\varepsilon_F; N)$ by DHOM, we rescale the single particle energy by factor $R_H = 0.7077$ so that $\varepsilon_F(\infty)$ reproduce the bulk value of Fermi energy of sodium. This rescaling is obtained if we set the density ρ of the model is $1.579 \times 10^{-2} \text{Å}^{-3}$. Of course the density in RBM is not rescaled.

In spite of crudeness of the models considered, Fig. 4 shows that reasonably good agreements with the experimental values are obtained, especially for DHOM. However we fail reproduce the irregular structures observed in the experiments (beginning from N =10 and 15).

5. Comment and discussion

We first consider the irregular structure just pointed out previously. For $N = 10$, the results obtained by molecular dynamical models[14,15] show that the equilibrium shape of the system slightly deviates from the axial symmetry whereas it keeps such symmetry in DHOM. The degrees of freedom of positive ions are partly included in the basis of the former model[14,15], while they are completely ignored in our models. Although we found one shape isomer with tri-axial symmetry at $N =$ 16, we neglect it during the present estimation, since its Fermi energy is much higher. Its contribution gives in the right direction to the theoretical results. As Fig. 1 shows, the complicated behavior of level splitting around $N = 16$ suggests that more careful investigation will be necessary in such region.

Both of the models we have considered so far are over simplified free electron gas in certain potential well. Hence it is desirable to deal with realistic model by taking into account of the residual interaction correctly. Unfortunately it is hard to carry out more consistent calculation, such as deformed Hartree-Fock calculation with tri-axially deformed basis. The many-body effects for a cluster system will be important when we investigate the even-odd staggering of other quantities, such as for example, the second difference of the total energy $\Delta_2 E$. We have calculated $\Delta_2 E$ by both two models and the results show clear even-odd staggering (figures are omitted). Roughly speaking, the strength of staggering is more prominent for RBM than DHOM. The magnitude of staggering in $\Delta_2 E$ will be reduced if we include the exchange effect.[17] An estimation in the local-spin-density approximation (LSDA) for the homogeneous electron gas by taking into account of the exchange and the correlation effects[18] gives the reduction is 30 to 40 % depending $r_s = 2$ to 6. After making such correction to $\Delta_2 E$, we find that about factor 0.8 strength of the effective average level distance still remains at given N for each model.

The authors would like to thank Prof. S. Bjørnholm, Prof. B. Mottelson, Prof. M. Manninen, Dr. O.B. Christensen and Dr. T. Døssing for many intensive discussions. Y.T. also thanks to Dr. S. Frauendorf, Dr. V.V. Pashkevich for stimulating discussions at the early stage of this work and Prof. I. Hamamoto for critical comment. He is grateful to Prof. J. Bondorf for extending kind hospitality at Niels Bohr Institute (NBI). The most part of this work was done during the authors' stay at NBI.

1) W.A. de Heer et al.: Solid State Phys. **40**, eds. H. Ehrenreich et al. (Academic, New York, 1987) p. 93.
2) W.A. de Heer: Rev. Mod. Phys. **65** (1993) 611.
3) M.K. Kappers et al.: J. Chem. Phys. **84** (1986) 1863.
4) M.K. Kappers et al.: Chem. Phys. Lett. **43** (1988) 251.
5) M.L. Homer et al.: Z. Phys. D**22** (1991) 441.
6) Ph. Dugourd et al.: Chem. Phys. Lett. **197** (1992) 433.
7) M. Knickelbein: Chem. Phys. Lett. **192** (1992) 129.
8) K. Clemenger: Phys. Rev. B**32** (1985) 1359.
9) A. Bohr and B. Mottelson: Nuclear Structure Vol. I, *Single-Particle Motion* (W.A. Benjamin, New York, 1969) p. 220.
10) K. Selby et al.: Phys. Rev. b**40** (1989) 5417.
11) A. Bohr and B. Mottelson: Nuclear Structure Vol. II, *Nuclear Deformation* (W.A. Benjamin, New York, 1975) p. 677.
12) C. Kittel: Introduction to Solid State Physics, 4th ed. (John Wiley & Sons, New York, 1971) p. 248.
13) Y. Wang et al.: J. Chem. Phys. **86** (1987) 3493. ; D.M. Lindsay et al.: J. Chem. Phys. **86** (1987) 3500.
14) U. Röthlisberger and W. Andreoni: J. Chem. Phys. **94** (1991) 8129.
15) O.B. Christensen et al.: Phys. Rev. Lett. **66** (1991) 2219. ; O.B. Christensen: Ph.D. thesis (1991).
16) S. Frauendorf and V.V. Pashkevich: Z. Phys. D**22** Suppl. (1993) 98.
17) D.R. Snider and R.S. Sorbello: Surf. Science **143** (1984) 204.
18) M. Manninen : private communication.